Two- and Three-Pion Production without Annihilation in Antiproton-Proton Interactions at 2.4 and 2.9 GeV/c†

R. A. JESPERSEN, W. J. KERNAN, AND R. A. LEACOCK
Department of Physics and Institute for Atomic Research, Iowa State University, Ames, Iowa 50010

(Received 10 November 1969)

A study was made of the reaction $\bar{p}p\to\bar{p}p\pi^+\pi^+$. The cross section for this reaction is 1.50±0.07 mb at 2.4 GeV/c and 2.57±0.10 mb at 2.9 GeV/c. The data at both momenta are consistent with nearly 100% $\bar{\Delta}^{--}\Delta^{++}$ double-resonance production. The reaction is peripheral at both momenta, the distribution of the c.m. scattering angle between the incoming $\bar{p}$ and the outgoing $\bar{p}\pi^-$ system being peaked at small angles. The $\rho_{1,1}$ spin-density matrix element has strong dependence on Δ^2, the square of the four-momentum transfer from the incoming $\bar{p}$ to the outgoing $\bar{p}\pi^-$ system. The joint spin-density matrix elements indicate no correlation between the $\bar{\Delta}^{--}$ and Δ^{++} production at either momentum. Calculations using the double-isobar one-pion-exchange model with form factors are compared to the data. The reactions $\bar{p}p\to\bar{p}p\pi^+\pi^-\pi^0$, $\bar{p}n\pi^+\pi^+\pi^-$, and $\bar{n}p\pi^-\pi^-\pi^+$ have cross sections of 10±5, 14±10, and 17±10 μb, respectively, at 2.4 GeV/c The corresponding values at 2.9 GeV/c are 124±40, 143±70, and 127±70 μb.

I. INTRODUCTION

MULTIPLE-PION production without annihilation in antiproton-proton interactions has been reported in bubble-chamber experiments at antiproton laboratory momenta of 1.6 to 2.2,[1] 2.5,[2] 2.7,[3] 2.8,[4] 3.28 and 3.66,[5] 3.6,[6] 5.7,[7,8] and 7.0[9] GeV/c. The cross section for the double-pion production reaction

$$\bar{p}p\to\bar{p}p\pi^+\pi^- \qquad (1)$$

is found to increase rapidly with beam momentum from 0.17 mb at 1.96 GeV/c to a maximum of 3.8 mb at 3.6 GeV/c, then decrease slowly. A prominent feature of reaction (1) at all of the above momenta is the dominance of the intermediate quasi-two-body reaction

$$\bar{p}p\to\bar{\Delta}^{++}(1236)\Delta^{++}(1236). \qquad (2)$$

The one-pion-exchange (OPE) model calculations for this reaction at 2.7 GeV/c were found[2] to give reasonably good predictions of the $p\pi^+$ and $\bar{p}\pi^-$ invariant-mass distributions and of the distribution of Δ^2, the four-momentum transfer from the incoming $\bar{p}$ to the outgoing $\bar{p}\pi^-$ system. However, the model did not predict the decay angular distributions correctly, and the $\rho_{1,1}$ spin-density matrix element was found to have a strong Δ^2 dependence not explained by the model.

Presented here is an investigation of reaction (1) at 2.4 and 2.9 GeV/c and comparisons of the intermediate reaction (2) with the OPE model predictions. Also presented are the cross sections for the triple-pion production reactions

$$\bar{p}p\to\bar{p}p\pi^+\pi^-\pi^0, \qquad (3)$$

$$\bar{p}p\to\bar{p}n\pi^+\pi^+\pi^-, \qquad (4)$$

$$\bar{p}p\to\bar{n}p\pi^-\pi^-\pi^+. \qquad (5)$$

Preliminary reports of this investigation at 2.9 GeV/c[10,11] and of other final states in these experiments[12] have been presented elsewhere.

The experimental procedure is discussed in Sec. II, and the experimental results are given in Sec. III.

† Based in part on a Ph.D. thesis submitted by R. A. Jespersen to Iowa State University, Ames, Ia. Work performed in part in the Ames Laboratory of the U.S. Atomic Energy Commission, Contribution No. 2650.

[1] C. Thornton Murphy, J. W. Chapman, R. Green, and J. Lys, Bull. Am. Phys. Soc. **13**, 1641 (1968); R. W. Green, J. W. Chapman, J. Lys, C. T. Murphy, and J. C. VanderVelde, *ibid.* **14**, 126 (1969); also C. T. Murphy (private communication).

[2] P. Mason, H. Muirhead, A. Poppleton, K. Whiteley, R. Rigopoulos, P. Tsilimigras, and A. Vayaki-Serafimidu, in Proceedings of the Lund International Conference on Elementary Particles, 1969, Lund, Sweden (unpublished).

[3] H. B. Crawley, R. A. Leacock, and W. J. Kernan, Phys. Rev. **154**, 1264 (1967); this paper is hereafter referred to as CLK.

[4] T. C. Bacon, F. Bomse, T. B. Borak, T. B. Cochran, W. J. Fickinger, E. R. Goza, H. W. K. Hopkins, and E. O. Salant, Phys. Rev. Letters **22**, 43 (1969). The reaction reported here is $\bar{p}p(n)\to\bar{p}p\pi^+\pi^-(n)$, using a deuterium target.

[5] T. Ferbel, J. Sandweiss, H. D. Taft, M. Gailloud, T. E. Kalogeropoulos, T. W. Morris, and R. M. Lea, Phys. Rev. Letters **9**, 351 (1962); T. Ferbel, A. Firestone, J. Sandweiss, H. D. Taft, M. Gailloud, T. W. Morris, W. J. Willis, A. H. Backmann, P. Baumel, and R. M. Lea, Phys. Rev. **138**, B1528 (1965).

[6] H. C. Dehne, E. Raubold, P. Söding, M. W. Teucher, G. Wolf, and E. Lohrmann, Phys. Letters **9**, 185 (1964); H. C. Dehne, E. Lohrmann, E. Raubold, P. Söding, M. W. Teucher, and G. Wolf, Phys. Rev. **136**, B843 (1964); K. Böckmann, B. Nellen, E. Paul, I. Borecka, J. Diaz, U. Heeren, U. Liebermeister, E. Lohrmann, E. Raubold, P. Söding, S. Wolff, S. Coletti, J. Kidd, L. Mandelli, V. Pelosi, S. Ratti, and L. Tallone, Phys. Letters **15**, 356 (1965).

[7] K. Böckmann, B. Nellen, E. Paul, B. Wagini, I. Borecka, J. Diaz, U. Heeren, U. Liebermeister, E. Lohrmann, E. Raubold, P. Söding, S. Wolff, J. Kidd, L. Mandelli, L. Mosca, V. Pelosi, S. Ratti, and L. Tallone, Nuovo Cimento **42**, 954 (1966).

[8] V. Alles-Borelli, B. French, Å. Frisk, and L. Michejda, Nuovo Ciemento **47A**, 232 (1967); **48A**, 360 (1967).

[9] T. Ferbel, A. Firestone, J. Johnson, J. Sandweiss, and H. D. Taft, Nuovo Cimento **38**, 19 (1965).

[10] R. A. Jespersen, W. J. Kernan, and R. A. Leacock, Bull. Am. Phys. Soc. **14**, 181 (1969); R. A. Jespersen, W. J. Kernan, and R. A. Leacock, in Proceedings of the Lund International Conference on Elementary Particles, 1969, Lund, Sweden (unpublished).

[11] W. J. Kernan, H. B. Crawley, R. A. Jespersen, and R. A. Leacock, Phys. Rev. D **1**, 48 (1970).

[12] R. P. Radlinski and W. J. Kernan, in Procedings of the Lund International Conference on Elementary Particles, 1969, Lund, Sweden (unpublished).

TABLE I. Numbers of events accepted.

	2.4 GeV/c	2.9 GeV/c
$\bar{p}p\pi^+\pi^-$	897	1015
$\bar{p}p\pi^+\pi^-\pi^0$	6	46
$\bar{p}n\pi^+\pi^+\pi^-$	8	53
$\bar{n}p\pi^-\pi^-\pi^+$	10	47

These results are compared with the predictions of the OPE model in Sec. IV, and the investigation is summarized in Sec. V.

II. EXPERIMENTAL PROCEDURE

The Brookhaven National Laboratory 31-in. hydrogen bubble chamber was exposed to an electrostatically separated beam of 2.9-GeV/c antiprotons and, subsequently, to one of 2.4 GeV/c. In tuning the beam, a clear separation of the pions, kaons, and antiprotons was seen at both momenta, ensuring that a reasonably pure sample of antiprotons reached the bubble chamber. In addition, the purity of the beam was monitored by a Čerenkov counter, which recorded pions and muons. At each momentum, this procedure resulted in a beam which was estimated to be more than 99% antiprotons, and no corrections were made for beam contamination. The beam flux was determined by counting the number of beam tracks entering the fiducial volume in every tenth frame of the film. The flux was found to be 8.8 beam tracks per picture at each momentum. The beam momenta were determined to be 2375±75 and 2885±80 MeV/c for the two data samples.

Approximately 60 000 pictures at the lower momentum and 40 000 at the higher were scanned for four-prong events, resulting in samples of 18 000 and 10 000 events, respectively, in the fiducial volume used. Approximately 10 000 pictures at each momentum were scanned a second time to determine the efficiency of locating four-prong events. It was determined that the first scan was 88% efficient at 2.4 GeV/c and 92% at 2.9 GeV/c. The events were measured in three stereoscopic views, reconstructed in space, and then kinematically fitted. An attempt was made to fit each event to all mass hypotheses for four or five particles in the final state consistent with the selection rules of the strong interactions. An event was said to have a fit to reaction (1) if the missing mass differed from zero by less than 4 standard deviations and if χ^2 was less than 31. An event was said to have a fit to any of the reactions (3) through (5) if the missing mass differed from the mass of the postulated neutral particle by less than 4 standard deviations and if χ^2 was less than 13. It was found that using more restrictive criteria eliminated real fits, while less restrictive ones merely included more simulated fits in the data samples.

TABLE II. Cross sections.

	2.4 GeV/c	2.9 GeV/c
$\bar{p}p\pi^+\pi^-$	1.50±0.07 mb	2.57±0.10 mb
$\bar{p}p\pi^+\pi^-\pi^0$	10±5 μb	124±40 μb
$\bar{p}n\pi^+\pi^+\pi^-$	14±10 μb	143±70 μb
$\bar{n}p\pi^-\pi^-\pi^+$	17±10 μb	127±70 μb

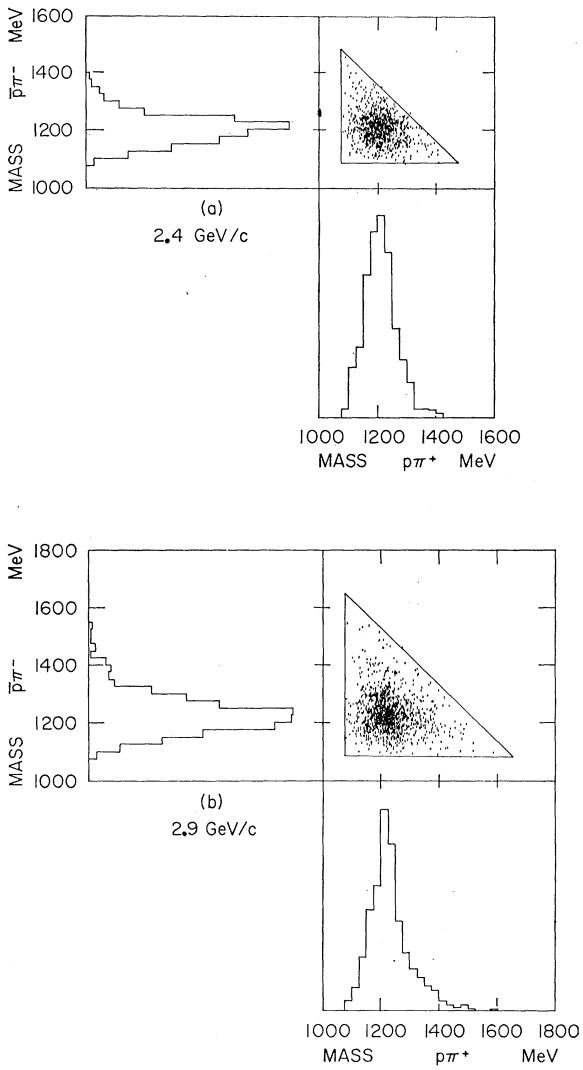

FIG. 1. Scatter plots of the $p\pi^+$ versus $\bar{p}\pi^-$ invariant-mass distributions. The kinematic limits are indicated by the solid lines. The figures are based on 897 events at 2.4 GeV/c and 1015 events at 2.9 GeV/c.

Each event which had a fit to any of reactions (1), (3), (4), or (5) was checked for ionization consistence of all outgoing tracks. This proved to be a strong requirement for reactions (1) and (3). It was possible to positively identify either the proton or the antiproton in more than 90% of the events having

TABLE III. Fractions of zero-, single-, and double-resonance production and the associated mass and width.

	2.4 GeV/c Fitted value	2.4 GeV/c Best estimate	2.9 GeV/c Fitted value	2.9 GeV/c Best estimate
$\alpha(\bar{p}\pi^- p\pi^+)$	0.17±0.04	0.10±0.10	0.06±0.01	0.05±0.05
$\alpha(\bar{\Delta}p\pi^+)=\alpha(\bar{p}\pi^-\Delta)$	0.00±0.01	0.00±0.05	0.00±0.02	0.00±0.02
$\alpha(\bar{\Delta}\Delta)$	0.83±0.04	0.90±0.10	0.94±0.02	0.95±0.05
Γ_0 (MeV)	128±7	120±8	126±3	120±8
ω_0 (MeV)	1213±2	1221±8	1220±1	1231±8

fits to reaction (1) at both 2.4 and 2.9 GeV/c. For events having fits to both reactions (1) and (3) or more than one fit to either of these reactions, this identification was usually sufficient to eliminate the ambiguities. No fits to reactions (1) and (3) were ambiguous with fits to reactions (4) or (5).

Although nearly every event which had a fit to reaction (1) was accepted as being due to that reaction, there were many simulated fits to reactions (3)–(5), where one particle was unmeasured. In particular, events due to reaction (1) frequently had simulated fits to reaction (3) in which the c.m. momentum of the fitted π^0 was close to zero. So an additional requirement for acceptance of fits to reaction (3) was that the c.m. momentum of the π^0 be greater than 100 MeV/c. It was also required that the missing mass be within 0.024 (GeV)^2 of the square of the π^0 mass, and that χ^2 be less than 2.0. These cuts were determined from examination of a scatter plot of the χ^2 versus missing-mass-squared distributions for all fits to reaction (3). These requirements, applied to all reaction-(3) fits, eliminated all ambiguities which had remained among the ionization-consistent fits to reactions (1) and (3).

Many of the reaction-(4) and -(5) events, for which only one of the two nucleons is observable, had no positively identifiable antiproton or proton. For these reactions there was a much greater degree of ambiguity than for the others. In order to determine which fits were real, an attempt was made to estimate the χ^2 and missing-mass-squared distributions to be expected from fits to reactions with an unseen nucleon. This study consisted of reprocessing all the 2.9-GeV/c events which had been accepted as due to reaction (1). Fits were attempted to the reactions

$$\bar{p}p\rightarrow\bar{p}(p)\pi^+\pi^-, \tag{6}$$

$$\bar{p}p\rightarrow(\bar{p})p\pi^+\pi^-, \tag{7}$$

where the particles in parentheses were treated as unmeasured. These were taken to be good approximations to reactions (4) and (5), respectively, in the sense of having a particle of similar mass and momentum unmeasured. It was found by examining scatter plots of χ^2 versus missing mass squared that 88% of the reaction (6) events had missing mass squared differing from the square of the proton mass by less than 0.16 (GeV)^2 and had χ^2 less than 2.0. The corresponding values for reaction (7) were 0.12 (GeV)^2 and 4.0, the differences being due to the tendency of the former reaction to have a high-momentum antiproton, while the latter more often has a low-momentum proton. These values were then used (along with ionization consistence) as the criteria for acceptance of fits to reactions (4) and (5), respectively, at both 2.4 and 2.9 GeV/c. It was estimated that the events with accepted fits to reactions (3), (4), or (5) constitued approximately 90% of all the measured events due to those reactions.

Fits which passed all of the above requirements were subjected to one final test. In order to eliminate fits which were not associated with true beam tracks or which resulted from poorly measured events, restrictions were made on the momentum and angles of the incident beam particle. These restrictions were determined from examination of the corresponding distributions for all four-prong events. The momentum was required to be within 165 MeV/c of the appro-

TABLE IV. Independent spin-density matrix elements. The values from the 2.7-GeV/c data are included here because of an error in CLK. In particular, the values of ρ_{nm} given in CLK on p. 1268 are incorrect.

	2.4 GeV/c	2.7 GeV/c	2.9 GeV/c	OPE model Prediction	OPE model Agreement
$\rho_{1,1}$	0.323±0.013	0.348±0.015	0.308±0.013	0.5	bad
$\mathrm{Re}\rho_{3,1}$	−0.033±0.014	−0.002±0.015	−0.026±0.012	0.0	fair
$\mathrm{Re}\rho_{3,-1}$	−0.028±0.014	−0.038±0.016	−0.026±0.014	0.0	fair

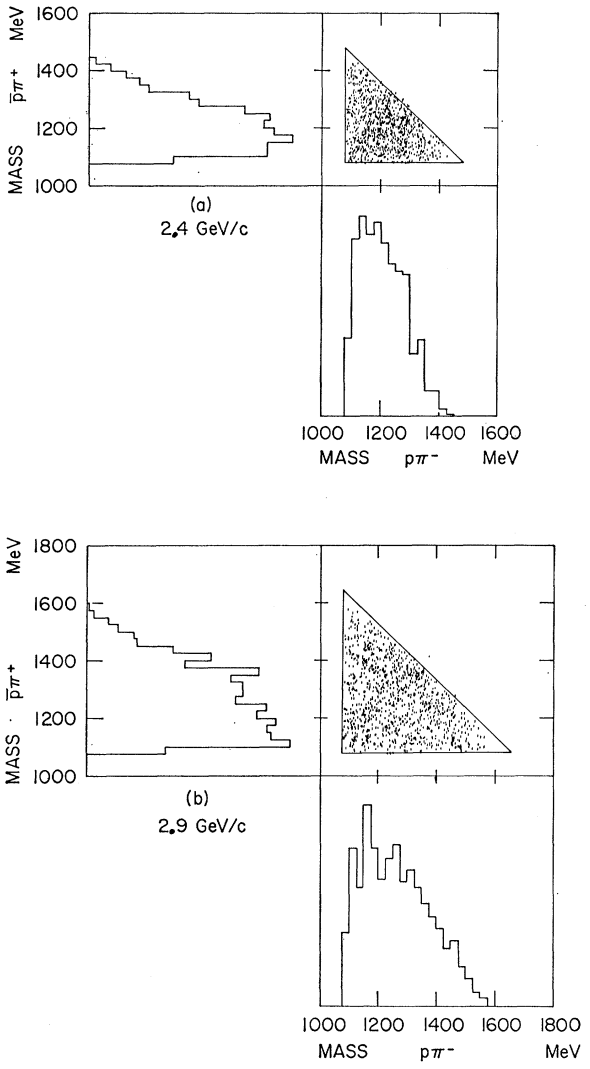

FIG. 2. Scatter plots of the $p\pi^-$ versus $\bar{p}\pi^+$ invariant-mass distributions.

priate value reported above for each data sample. The dip was required to be within 5° of zero, and the azimuth was required to be within 1.5° of the average value of the distribution as a function of the vertex position along the incident beam direction. These restrictions eliminated 1.6% of the accepted fits to reaction (1) at both momenta. It was assumed that this factor applied to all other final states as well, and the beam track count used for determining the cross sections was reduced by 1.6%. In Table I are shown the numbers of events accepted as due to reactions (1), (3), (4), and (5) at each momentum.

Approximately 40–45 events at each momentum had an identified $\bar{p}$ or p but no acceptable fit to any of reactions (1), (3), (4), or (5). These events were considered to be due to reaction (1) for the purpose of cross-section calculations, since statistics favor this over the other reactions in which there is a $\bar{p}$ or p in the final state. These events, along with the reaction-(1) events not found in the scanning, account for a significant fraction of all the reaction-(1) events, and indicate the possibility of biases in the final data samples. This possibility was examined by looking for apparent violations of C or CP invariance in all of the distributions examined which are subject to such tests. The specific distributions examined are listed in CLK. All of the requirements are satisfied within statistical limits at both beam momenta, indicating that the final data samples for reaction (1) are unbiased in this respect.

III. EXPERIMENTAL RESULTS

A. Cross Sections

The cross sections for reactions (1), (3), (4), and (5) are given in Table II. The numbers of events due to reactions (3)–(5) are so small that no further study of these reactions was attempted. The remainder of this paper is devoted to the investigation of reaction (1).

B. Invariant-Mass Distributions and Resonance Production

Figure 1 shows the two-dimensional scatter plots of the invariant masses of the outgoing $\bar{p}\pi^-$ and $p\pi^+$ combinations. Each of these mass distributions is

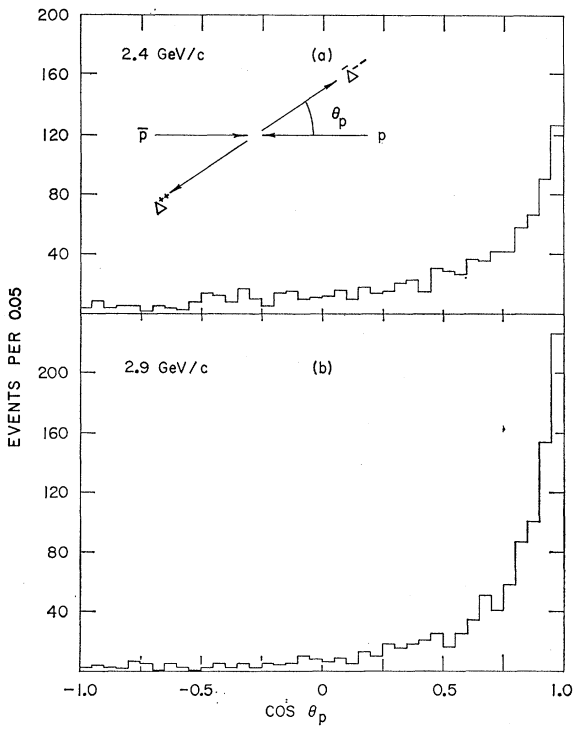

FIG. 3. Center of mass production angular distributions.

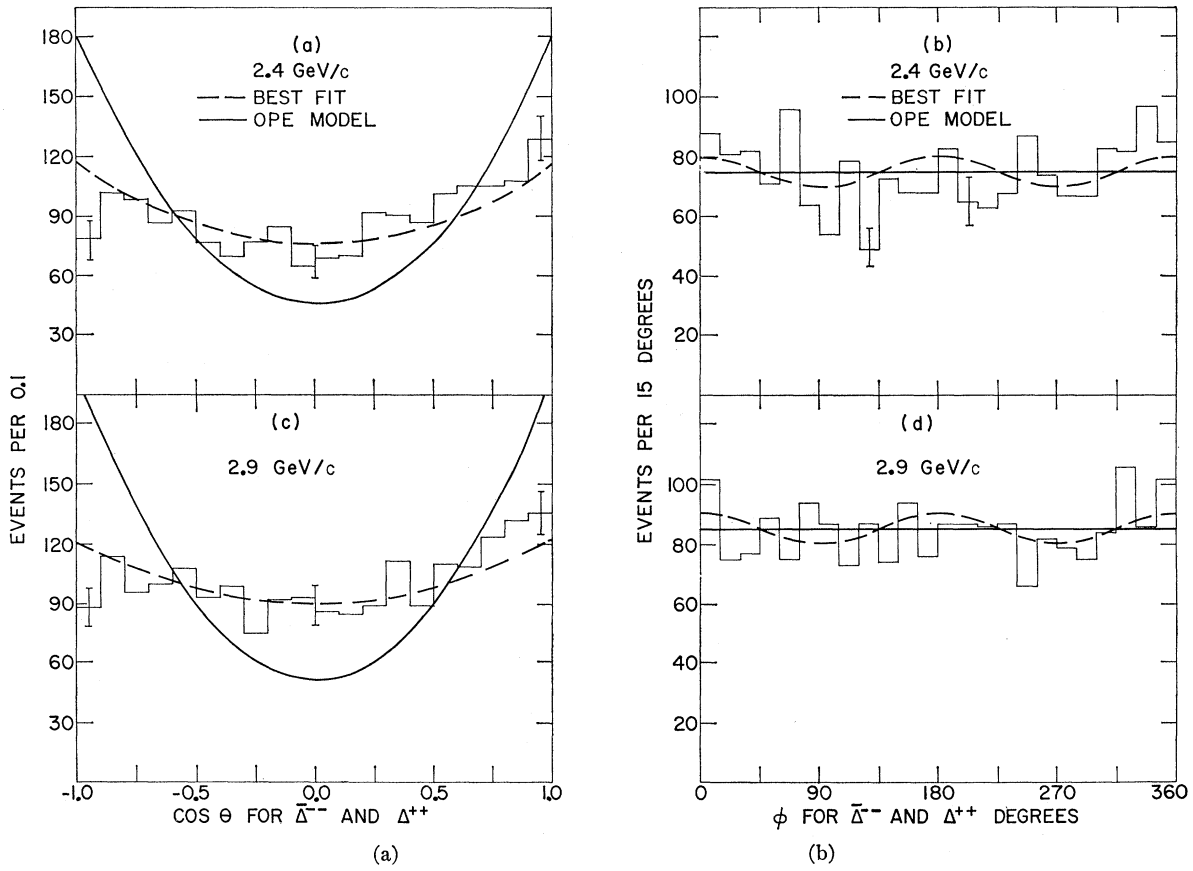

FIG. 4. (a) and (c): $\cos\theta$ distributions, where θ is the polar angle between the incoming $\bar{p}$ (p) and the outgoing $\bar{p}$ (p) momenta in the rest frame of the outgoing $\bar{p}\pi^-$ ($p\pi^+$) system. (b) and (d): ϕ distributions, where ϕ is the azimuthal angle corresponding to θ. Each event appears twice (C invariance invoked). The dashed curves are plots of Eqs. (11) and (12), using the density-matrix elements obtained from the data. The solid curves are predictions of the double-isobar OPE model. All curves are normalized to the data.

strongly peaked at about 1220 MeV. The clustering of each scatter plot about the overlap region shows the dominance of simultaneous resonance production at both 2.4 and 2.9 GeV/c, i.e., reaction (1) proceeds primarily through the intermediate reaction (2).

In order to determine just what fraction of the reaction goes through this intermediate state at each momentum, fits were done to the scatter plots of Fig. 1. Since the resonances can be produced doubly, singly, or not at all, the theoretical expression for these invariant-mass distributions was written as a sum of expressions for each of these possibilities. The form used is

$$L(\bar{\omega},\omega)=\alpha(\bar{p}\pi^-p\pi^+)F(\bar{p}\pi^-p\pi^+)+\alpha(\bar{\Delta}p\pi^+)F(\bar{\Delta}p\pi^+)+\alpha(\bar{p}\pi^-\Delta)F(\bar{p}\pi^-\Delta)+\alpha(\bar{\Delta}\Delta)F(\bar{\Delta}\Delta). \quad (8)$$

In this expression, $\bar{\omega}$ (ω) is the invariant mass of the outgoing $\bar{p}\pi^-$ ($p\pi^+$) combination, the α's are the fractions of the events of the types indicated by the arguments [e.g., $\alpha(\bar{\Delta}\Delta)$ is the fraction of reaction (1) going through the intermediate reaction (2)], and the F's are phenomenological expressions representing the production and decay of the state indicated by the arguments [e.g., $F(\bar{\Delta}\Delta)$ represents phase-space production of a $\bar{\Delta}^{--}\Delta^{++}$ state followed by Breit-Wigner decay of that state to $\bar{p}\pi^-p\pi^+$]. The forms of these functions are given in CLK, where the fitting procedure is described in detail. The form of the energy-dependent width used in the Breit-Wigner shapes is

$$\Gamma(\omega)=\Gamma_0\left(\frac{P(\omega;M^2,m^2)}{P(\omega_0;M^2,m^2)}\right)^3\left[\frac{Am^2+[P(\omega_0;M^2,m^2)]^2}{Am^2+[P(\omega;M^2,m^2)]^2}\right]. \quad (9)$$

The quantity in the large square brackets is an empirical correction factor. The form of this factor is from nuclear reactions theory, and the parameter $A=2.2$ is from a phase-shift fit by Anderson as presented by Jackson.[13] Physically, $(Am^2)^{-1/2}$ is the radius of interaction of the $p\pi^+$ (or $\bar{p}\pi^-$) system. Γ_0 is the width parameter, with Anderson's fit resulting in the value 123 MeV.[14]

[13] J. D. Jackson, Nuovo Cimento **34**, 1644 (1964).

[14] Jackson notes that Gell-Mann and Watson choose $A=1.3$ and $\Gamma_0=116$ MeV. In the present study, this value of A improves the fit slightly, but then a somewhat larger Γ_0 is preferred.

TABLE V. Joint spin-density matrix elements. The values from the 2.7-GeV/c data of CLK are presented here because they were not previously calculated.

	2.4 GeV/c	2.7 GeV/c	2.9 GeV/c	OPE model Prediction	OPE model Agreement
$\frac{1}{2}(\rho_{--}^{3,3}-\rho_{--}^{1,1})$	0.052±0.045	0.033±0.050	0.086±0.042	0.25	bad
$\mathrm{Re}\rho_{--}^{3,1}$	−0.002±0.045	0.014±0.052	0.004±0.040	0.0	good
$\mathrm{Re}\rho_{3,1}^{--}$	0.034±0.045	−0.010±0.051	0.020±0.043	0.0	good
$\mathrm{Re}\rho_{--}^{3,-1}$	0.048±0.048	0.063±0.054	0.022±0.043	0.0	fair
$\mathrm{Re}\rho_{3,-1}^{--}$	0.107±0.046	0.000±0.052	−0.020±0.044	0.0	fair
$\mathrm{Re}(\rho_{3,1}^{3,1}-\rho_{3,1}^{-1,-3})$	−0.010±0.031	−0.019±0.036	−0.053±0.029	0.0	fair
$\mathrm{Re}(\rho_{1,3}^{3,1}-\rho_{1,3}^{-1,-3})$	0.030±0.031	0.017±0.035	0.019±0.028	0.0	good
$\mathrm{Re}(\rho_{3,1}^{3,-1}+\rho_{3,1}^{1,-3})$	0.028±0.033	0.040±0.038	0.079±0.031	0.0	fair
$\mathrm{Re}(\rho_{1,3}^{3,-1}+\rho_{1,3}^{1,-3})$	−0.004±0.032	0.039±0.036	0.027±0.032	0.0	fair
$\mathrm{Re}(\rho_{3,-1}^{3,1}-\rho_{3,-1}^{-1,-3})$	0.018±0.034	0.035±0.037	0.007±0.030	0.0	good
$\mathrm{Re}(\rho_{-1,3}^{3,1}-\rho_{-1,3}^{-1,-3})$	−0.026±0.033	0.089±0.037	0.000±0.031	0.0	fair
$\mathrm{Re}(\rho_{3,-1}^{3,-1}+\rho_{3,-1}^{1,-3})$	0.004±0.035	0.062±0.040	0.038±0.033	0.0	fair
$\mathrm{Re}(\rho_{-1,3}^{3,-1}+\rho_{-1,3}^{1,-3})$	−0.016±0.035	−0.010±0.039	−0.026±0.034	0.0	good

A similar fitting procedure was used by Alles-Borelli *et al.*[8] at 5.7 GeV/c. The calculations of the $p\pi^+$ and $\bar{p}\pi^-$ invariant-mass distributions using the parameters of the fit were found to be good representations of their data. This is not the case for the 2.4- and 2.9-GeV/c data, however. Apparently the expressions used in the fit are not adequate this close to the $\bar{\Delta}\Delta$ threshold. The calculated $p\pi^+$ and $\bar{p}\pi^-$ mass distributions using the parameters of the fit are peaked slightly below the peaks in the data. Similar difficulties were noted at 2.7 GeV/c.[15]

To see if a better fit to the histograms could be obtained, the empirical correction factor A occurring in the resonance-width expression (9) was used as an additional adjustable parameter in the fitting procedure. The fits to the data at 2.4, 2.7, and 2.9 GeV/c were found to be sensitive to the value of A; in each case the fits resulted in values of A near (but not equal to) zero. With A approximately zero (corresponding to a very long radius of interaction), the calculated distribution with nearly 100% double-resonance production is a better representation of the data at each momentum than is the corresponding "best fit" with A fixed at 2.2.

In fitting the 2.4-GeV/c data, there is yet another difficulty besides the form of the theoretical distribution. The kinematics require that the $p\pi^+$ and $\bar{p}\pi^-$ invariant masses be in or very near the $\bar{\Delta}^{--}\Delta^{++}$ region. Consequently, zero- and single-resonance production can contribute only to this region. This results in the fit to the theoretical distribution of expression (8) being rather insensitive to the fractions of zero-, single-, and double-resonance production.

Because of all of these uncertainties "best estimates" of the parameters are given along with the fitted values. These estimates were based in part on the above discussion of the fitting. Also considered were plots of the $\bar{p}\pi^-$ and $p\pi^+$ invariant-mass distributions for events in various Δ^2 bins. It is shown below that there is strong Δ^2 dependence in the interaction. Events which do not involve double-resonance production might be found by examination of these mass distributions as functions of Δ^2. The scatter plots of the $\bar{p}\pi^-$ versus the $p\pi^+$ invariant-mass distributions binned on Δ^2 show very pronounced clustering of the events in the $\bar{\Delta}^{--}\Delta^{++}$ region at small Δ^2. This clustering becomes less pronounced with increasing Δ^2, owing, at least in part, to kinematic effects. From these scatter plots it is clear that double-resonance production accounts for nearly 100% of the events at small Δ^2, but it is difficult to make a conclusion concerning the amount of nonresonant background at large Δ^2. Calculations using the OPE model (Sec. IV) indicate, however, that even the events at large Δ^2 are consistent with nearly 100% $\bar{\Delta}^{--}\Delta^{++}$ production at both momenta.

The best estimates based on these considerations are that the double-resonance production is nearly 100% at both 2.4 and 2.9 GeV/c, any background being entirely nonresonant. The estimated resonance masses are the values which give peaks in the calculated distributions corresponding to the peaks in the data. These estimates are shown along with the results of the four-parameter fits in Table III. The errors quoted for the fitted values are purely statistical and do not reflect uncertainties in the forms used for the functions F.

In contrast to the resonance production shown in Fig. 1, there is no evidence for $\bar{\Delta}^0(1236)$ or $\Delta^0(1236)$ in the $\bar{p}\pi^+$ and $p\pi^-$ invariant-mass distributions of Fig. 2. The distributions are smooth, and there is no clustering in the scatter plots. All other invariant-mass distributions were also examined, and no evidence for resonable production was seen in any of

[15] H. B. Crawley, Ph.D. thesis, Iowa State University of Science and Technology, 1966 (unpublished).

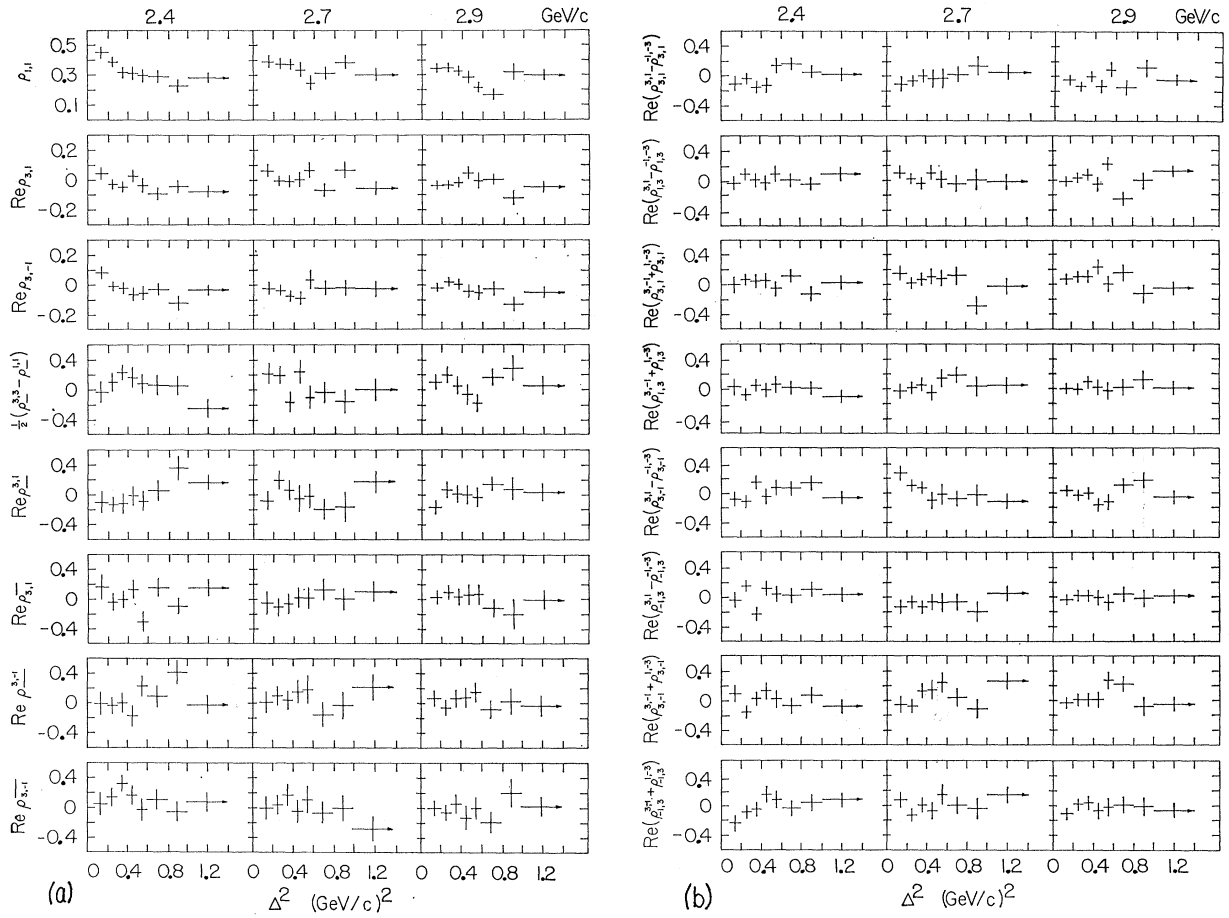

FIG. 5. Spin-density matrix elements as functions of Δ^2, the square of the four-momentum transfer from the incident $\bar{p}$ to the outgoing $\bar{p}\pi^-$ system. Each event appears twice in the independent density-matrix elements $\rho_{1,1}$, Re $\rho_{3,1}$, and Re $\rho_{3,-1}$. The data at 2.7 GeV/c are presented here because the data (but not the solid curves) shown in Fig. 6 of CLK are incorrect. The joint density-matrix elements at 2.7 GeV/c are also shown here because they were not previously calculated.

them (as would be expected for the case of 100% $\bar{\Delta}^{--}\Delta^{++}$ production). No known resonances decaying to $\pi^+\pi^-$ are energetically possible at 2.4 GeV/c, and $\rho(765)$ is too close to the kinematic limit to be seen in the 2.9-GeV/c data. Discussion of the $\bar{p}\pi^+\pi^-$ and $p\pi^+\pi^-$ invariant-mass distributions at 2.7 and 2.9 GeV/c has been presented elsewhere.[11] Resonance effects were reported in these distributions by Bacon *et al.*[4] at 2.8 GeV/c. However, the conclusion in Ref. 11 is that the $\bar{p}\pi^+\pi^-$ and $p\pi^+\pi^-$ invariant-mass distributions are adequately explained, at least at 2.7 and 2.9 GeV/c, by the assumption of 100% $\bar{\Delta}^{--}\Delta^{++}$ production (see Sec. IV).

C. Production Angular Distributions

In the remainder of this paper, the above results are considered to be consistent with 100% $\bar{\Delta}^{--}\Delta^{++}$ double-resonance production at both 2.4 and 2.9 GeV/c. Comments are made at appropriate points to indicate the effects of adding a small nonresonant background. The distributions of the production angle θ_p at the two momenta are shown in Fig. 3. The reaction is seen to be peripheral at 2.4 GeV/c, with 38% of the events having $\cos\theta_p > 0.8$, and more strongly peripheral at 2.9 GeV/c, with 56% of the events having $\cos\theta_p > 0.8$. Previous experiments concerning this and other quasi-two-body interactions have shown this tendency of the forward peak to become narrower with increasing beam momentum.[16] An interpretation of the peripheral character of the reaction is given in Sec. IV.

D. Decay Angular Distributions and Density-Matrix Elements

The general form of the angular distribution of the $\bar{\Delta}^{--}$ (Δ^{++}) decay products in the $\bar{\Delta}^{--}$ (Δ^{++}) rest

[16] G. Wolf, Phys. Rev. Letters **19**, 925 (1967).

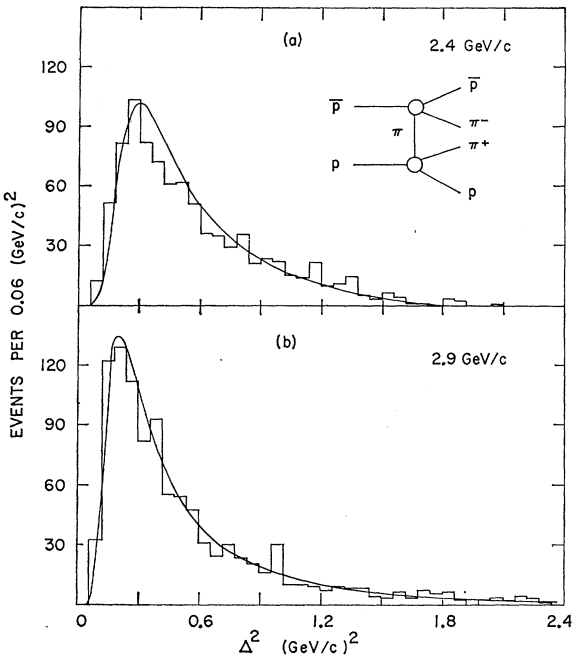

FIG. 6. Δ^2 distributions, where Δ^2 is the square of the four-momentum transfer from the incident $\bar{p}$ to the outgoing $\bar{p}\pi^-$ system. The solid curves are the predictions of the double-isobar OPE model normalized to the data. The Feynman diagram for this model is shown in (a).

frame can be written as[17]

$$W(\cos\theta, \varphi) = C[(\tfrac{1}{2}-\rho_{1,1})\sin^2\theta + \rho_{1,1}(\tfrac{1}{3}+\cos^2\theta) - (2/\sqrt{3})\,\mathrm{Re}\rho_{3,-1}\sin^2\theta\cos 2\varphi - (2/\sqrt{3})\,\mathrm{Re}\rho_{3,1}\sin 2\theta\cos\varphi], \quad (10)$$

where C is a normalization constant, θ is the angle between the incident $\bar{p}$ (p) and the outgoing $\bar{p}$ (p) in the $\bar{\Delta}^{--}$ (Δ^{++}) rest frame, and φ is the corresponding azimuthal angle. The ρ's are the spin-density matrix elements for the Δ in the θ, φ coordinate system.

The individual $\cos\theta$ and φ distributions are obtained from expression (10) by integration over φ and $\cos\theta$, respectively:

$$W_1(\cos\theta) = C_1[(\tfrac{3}{4}-\rho_{1,1}) + 3(\rho_{1,1}-\tfrac{1}{4})\cos^2\theta], \quad (11)$$

$$W_2(\varphi) = C_2[(1-4/\sqrt{3})\,\mathrm{Re}\rho_{3,-1}\cos 2\varphi], \quad (12)$$

where C_1 and C_2 are normalization constants. By multiplying these expressions by various trigonometric functions of θ and φ and integrating, it is possible to find the following expressions:

$$\rho_{1,1} = (15/8)\langle\cos^2\theta\rangle - \tfrac{3}{8}, \quad (13a)$$

$$\mathrm{Re}\rho_{3,1} = -\tfrac{5}{8}\sqrt{3}\langle\sin 2\theta\cos 2\varphi\rangle, \quad (13b)$$

$$\mathrm{Re}\rho_{3,-1} = -\tfrac{1}{2}\sqrt{3}\langle\cos 2\varphi\rangle. \quad (13c)$$

[17] K. Gottfried and J. D. Jackson, Nuovo Cimento **33**, 309 (1964).

Here $\langle f(\cos\theta, \varphi)\rangle$ denotes the average value of the function f. The density-matrix elements were calculated from expression (13) using the data for the $\bar{\Delta}^{--}$ and Δ^{++} decays combined (charge conjugation invoked). The results are shown in Table IV along with the predictions of the OPE model, which is discussed in Sec. IV. Inserting these values into expressions (11) and (12) gave the "best fits" to the data shown in Fig. 4. The fits to the $\cos\theta$ distributions are reasonably good, except for a tendency of the data at both 2.4 and 2.9 GeV/c to have more events near $\cos\theta = 1$ than near $\cos\theta = -1$. The fits to the φ distributions are not very good at either momentum. There are departures from isotropy, particularly at 2.4 GeV/c, but the calculation does not reproduce them very well. Further discussion of these distributions is given in Sec. IV.

Pilkuhn and Svensson[18] have pointed out that still more information about the decays can be found by

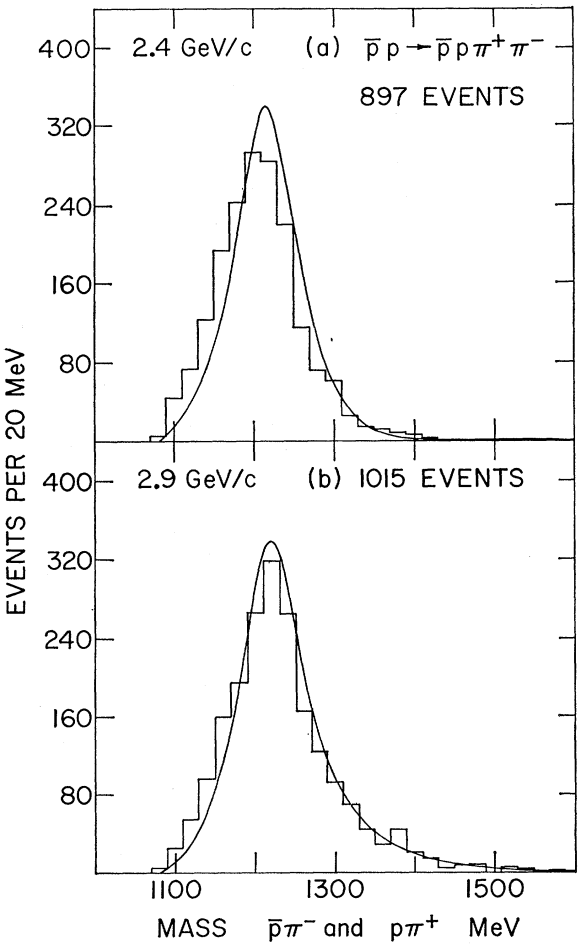

FIG. 7. Combined $p\pi^+$ and $\bar{p}\pi^-$ invariant-mass distributions. The solid curves are the predictions of the double-isobar OPE model normalized to the data.

[18] H. Pilkuhn and B. E. Y. Svensson, Nuovo Cimento **38**, 518 (1965).

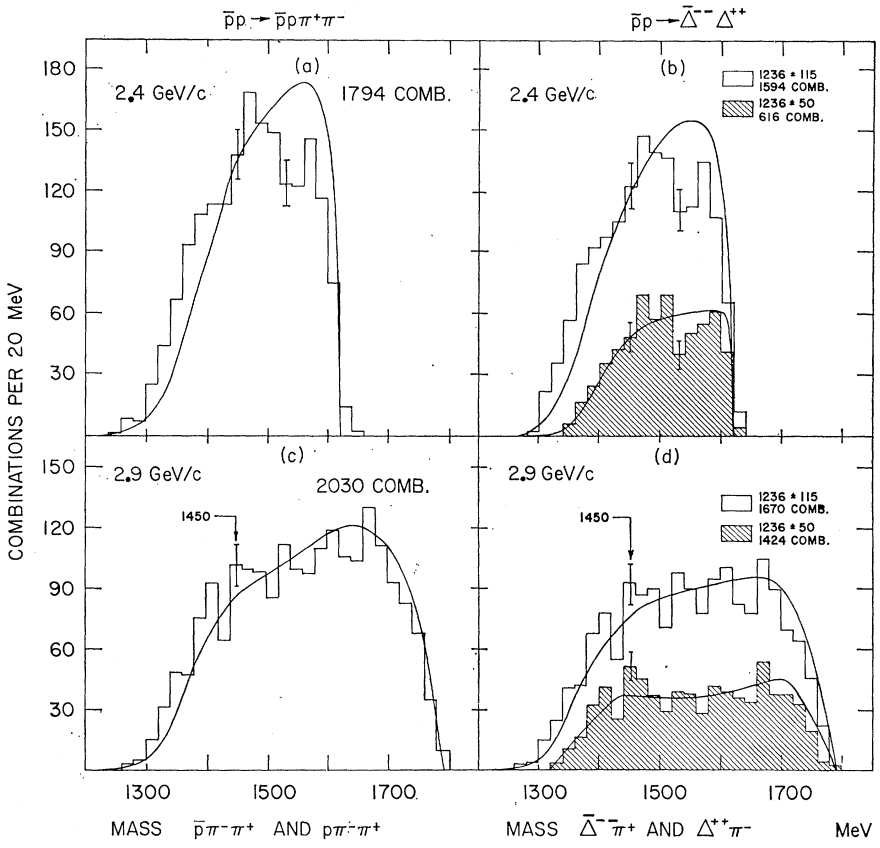

FIG. 8. (a) and (c): Combined $p\pi^-\pi^+$ and $\bar{p}\pi^-\pi^+$ invariant-mass distributions. (b) and (d): Same distributions for events having the $\bar{p}\pi^-$ and $p\pi^+$ invariant masses in the Δ region (defined as 1236 ± 115 MeV for the open histograms and 1236 ± 50 MeV for the shaded histograms). The solid curves are the predictions of the double-isobar OPE model normalized to the data.

examining the joint decay distribution $W(\cos\bar{\theta}, \cos\theta, \bar{\varphi}, \varphi)$, where $\bar{\theta}$, $\bar{\varphi}$ (θ, φ) are the decay angles of the $\bar{\Delta}^{--}$ (Δ^{++}). This allows the determination of 13 additional independent production amplitudes (but not the complete density matrix). The expressions[19] are

$$\tfrac{1}{2}(\rho_{--}^{3,3}-\rho_{--}^{1,1}) = (25/16)\langle(1-3\cos^2\bar{\theta})(1-3\cos^2\theta)\rangle, \quad (14a)$$

$$\mathrm{Re}\rho_{--}^{3,1} = -(25\sqrt{3}/16)\langle(1-3\cos^2\theta)\sin2\bar{\theta}\cos\bar{\varphi}\rangle, \quad (14b)$$

$$\mathrm{Re}\rho_{3,1}^{--} = -(25\sqrt{3}/16)\langle(1-3\cos^2\bar{\theta})\sin2\theta\cos\varphi\rangle, \quad (14c)$$

$$\mathrm{Re}\rho_{--}^{3,-1} = -(5\sqrt{3}/4)\langle(1-3\cos^2\theta)\cos2\bar{\varphi}\rangle, \quad (14d)$$

$$\mathrm{Re}\rho_{3,-1}^{--} = -(5\sqrt{3}/4)\langle(1-3\cos^2\bar{\theta})\cos2\varphi\rangle, \quad (14e)$$

$$\mathrm{Re}(\rho_{3,1}^{3,1}-\rho_{3,1}^{-1,-3}) = (225/96)\langle\sin2\bar{\theta}\sin2\theta\cos(\bar{\varphi}+\varphi)\rangle, \quad (14f)$$

$$\mathrm{Re}(\rho_{1,3}^{3,1}-\rho_{1,3}^{-1,-3}) = (225/96)\langle\sin2\bar{\theta}\sin2\theta\cos(\bar{\varphi}-\varphi)\rangle, \quad (14g)$$

$$\mathrm{Re}(\rho_{3,1}^{3,-1}+\rho_{3,1}^{1,-3}) = (15/8)\langle\sin2\theta\cos(2\bar{\varphi}+\varphi)\rangle, \quad (14h)$$

$$\mathrm{Re}(\rho_{1,3}^{3,-1}+\rho_{1,3}^{1,-3}) = (15/8)\langle\sin2\theta\cos(2\bar{\varphi}-\varphi)\rangle, \quad (14i)$$

$$\mathrm{Re}(\rho_{3,-1}^{3,1}-\rho_{3,-1}^{-1,-3}) = (15/8)\langle\sin2\bar{\theta}\cos(\bar{\varphi}+2\varphi)\rangle, \quad (14j)$$

$$\mathrm{Re}(\rho_{-1,3}^{3,1}-\rho_{-1,3}^{-1,-3}) = (15/8)\langle\sin2\bar{\theta}\cos(\bar{\varphi}-2\varphi)\rangle, \quad (14k)$$

$$\mathrm{Re}(\rho_{3,-1}^{3,-1}+\rho_{3,-1}^{1,-3}) = \tfrac{3}{2}\langle\cos2(\bar{\varphi}+\varphi)\rangle, \quad (14l)$$

$$\mathrm{Re}(\rho_{-1,3}^{3,-1}+\rho_{-1,3}^{1,-3}) = \tfrac{3}{2}\langle\cos2(\bar{\varphi}-\varphi)\rangle, \quad (14m)$$

where

$$\rho_{-}^{m,n} = \rho_{3,3}^{m,n}+\rho_{-3,-3}^{m,n}-\rho_{1,1}^{m,n}-\rho_{-1,-1}^{m,n},$$

$$\rho_{m,n}^{-} = \rho_{m,n}^{3,3}+\rho_{m,n}^{-3,-3}-\rho_{m,n}^{1,1}-\rho_{m,n}^{-1,-1}.$$

The values obtained from the data are given in Table V, where they are compared to the predictions of the OPE model (discussed in Sec. IV).

These matrix elements were also calculated as functions of Δ^2, the square of the four-momentum transfer from the incident $\bar{p}$ to the outgoing $\bar{p}\pi^-$ system. This was done by applying the method described above to the data in various Δ^2 bins. The results are shown in Fig. 5, and are discussed in Secs. IV and V.

IV. COMPARISON OF DATA WITH OPE MODEL

It was noted in Sec. III that reaction (1) is peripheral, particularly at 2.9 GeV/c. This indicates the possibility of interpreting the data using the OPE

[19] These expressions, derived by us, differ from those of Alles-Borelli *et al.* (Ref. 8) in some cases.

model. In this section, the OPE calculations are discussed and compared to the data.

The calculations presented here are based entirely on the contribution of the "double-isobar" diagram shown in Fig. 6. The $I_z=\frac{1}{2}$ diagram (obtained by interchanging the π^- and π^+ in Fig. 6) results in a contribution which is approximately 1% of that of the double-isobar diagram and hence is neglected. The two "Drell" diagrams, in which a π^0 is exchanged producing both final pions at the same vertex, can contribute only to zero- or single-resonance production. Since the data presented in Sec. III are interpreted as 100% double-resonance production, the contribution of the two Drell diagrams is neglected on empirical grounds. Also neglected are possible contributions from ρ meson exchange. The values of the spin-density matrix elements predicted by the double-isobar OPE model are $\rho_{1,1}=0.5$ and $\mathrm{Re}\rho_{3,1}=\mathrm{Re}\rho_{3,-1}=0$. The experimental results of Table IV disagree with this value of $\rho_{1,1}$ at all three momenta. An even more striking disagreement between the model and the data is the strong Δ^2 dependence of $\rho_{1,1}$ shown in Fig. 5. A calculation by Svensson[20] taking into account absorption by other possible final states accounts for a comparable effect in the data at 3.6 and 5.7 GeV/c. However, a similar calculation by Hite and Jackson as presented in CKL failed to reproduce the effect at 2.7 GeV/c.

Using the OPE model predictions for the density-matrix elements in expressions (11) and (12) results in the predicted distribution $W_1(\cos\theta)$ having the simple form $1+3\cos^2\theta$, while $W_2(\varphi)$ is independent of the azimuthal angle φ. These forms are compared with the data in Fig. 4. The agreement with the $\cos\theta$ distributions is seen to be very poor at both 2.4 and 2.9 GeV/c, and the φ distributions show deviations from isotropy, particularly at 2.4 GeV/c.

The OPE model predicts that all of the joint spin-density matrix elements given in expressions (14) are zero except for $\rho_{--}^{1,1}$ in (14a). The predicted value is $\frac{1}{2}(\rho_{--}^{3,3}-\rho_{--}^{1,1})=0.25$. The experimental value of this quantity shown in Table V does not agree with this prediction. This is to be expected because of the relationship of $\rho_{--}^{1,1}$ to $\rho_{1,1}$, which also differs from the prediction. All of the other joint density-matrix elements in Table V are in reasonably good agreement with the model, indicating little or no correlation in the $\bar{\Delta}^{--}$ and Δ^{++} production. Some Δ^2 dependence in a few of these terms is indicated in Fig. 5; however, most of these fluctuations are not statistically significant.

The OPE model predictions of the spin-density matrix elements do not depend on any form factors which may be used to account for the virtuality of the exchanged pion and other off-shell effects. For calculations which do depend on these quantities, the form factors of Dürr and Pilkuhn[21] as fitted by Wolf[16] were used. The differential cross section for reaction (1) is given by Eq. (7) of CLK, with the form factor Ω replaced by

$$\Omega(\bar{\omega},\omega,\Delta^2)=G^2(\Delta^2)\Lambda(\bar{\omega},\Delta^2)\Lambda(\omega,\Delta^2),$$

where

$$\Lambda(\omega,\Delta^2)=\frac{(\omega+M)^2+\Delta^2}{(\omega+M)^2-m^2}\left(\frac{P(\omega;M^2,-\Delta^2)}{P(\omega;M^2,m^2)}\right)^2\times\frac{1+R^2[P(\omega;M^2,m^2)]^2}{1+R^2[P(\omega;M^2,-\Delta^2)]^2}$$

and $G(\Delta^2)=(c-m^2)/(c+\Delta^2)$. Here $\bar{\omega}$ (ω) is the $\bar{p}\pi^-$ ($p\pi^+$) invariant mass and Δ^2 is the square of the four-momentum transfer from the incident $\bar{p}$ to the outgoing $\bar{p}\pi^-$ system. The empirical parameters c and R were determined by Wolf from a fit to the data for several reactions: $c=2.29\pm0.27$ (GeV)^2 and $R=2.97\pm0.11$ (GeV)$^{-1}$.

The double-isobar OPE model prediction of the differential cross section with respect to Δ^2 at each momentum is shown normalized to the data in Fig. 6. The agreement is seen to be very good at 2.9 GeV/c, even for large Δ^2. At 2.4 GeV/c, the calculated peak is slightly too broad, but is a reasonable representation of the data. The model prediction of the differential cross section with respect to ω at each momentum is shown normalized to the combined $\bar{p}\pi^-$ and $p\pi^+$ invariant-mass distributions in Fig. 7. The shapes of the calculated peaks are seen to be good representations of the data, but they are centered at slightly higher mass than are the data, particularly at 2.4 GeV/c. The phase-space predictions for these distributions are considerably broader than the double-isobar curves and are peaked at somewhat lower mass. The predictions of the double-isobar model were also compared with the combined $\bar{p}\pi^-$ and $p\pi^+$ invariant-mass distributions in various Δ^2 bins (not shown). The agreement was adequate in all Δ^2 bins at both momenta, supporting the conclusion of nearly 100% double-resonance production.

The double-isobar OPE model used above contains no free parameters; however, as mentioned, the predictions of the model were normalized to the data in the figures. The predictions of the model for the cross sections for $\bar{p}p\to\bar{\Delta}^{--}\Delta^{++}$ at 2.4, 2.7, and 2.9 GeV/c are 1.94, 2.60, and 2.82 mb, respectively, based on the double-isobar diagram alone. These are compared to the experimental cross sections for reaction (1) of 1.48 ± 0.07, 1.93 ± 0.16, and 2.53 ± 0.10 mb, respectively, at these momenta. It is seen that the energy dependence is roughly correct, but that the model predictions are too large by an over-all multiplicative constant (1.3 at 2.4 and 2.7 GeV/c, 1.1 at 2.9 GeV/c).

[20] B. E. Y. Svensson, Nuovo Cimento **39**, 667 (1965).

[21] H. P. Dürr and H. Pilkuhn, Nuovo Cimento **40A**, 899 (1965).

The double-isobar OPE model also predict the differential cross section with respect to u, the $p\pi^+\pi^-$ invariant mass. The $\bar{p}\pi^+\pi^-$ and $p\pi^+\pi^-$ invariant-mass distributions are identical within statistical limits and are shown combined in Fig. 8(a) at 2.4 GeV/c and 8(c) at 2.9 GeV/c. No outstanding enhancements are seen in the 2.9-GeV/c data or in those at 2.7 GeV/c,[11,15] although there are possible small effects at 2.7 GeV/c in the regions 1400–1450 MeV and 1600–1700 MeV. In the 2.4-GeV/c data there appears to be an effect in the region 1440–1520 MeV.

The presence of a resonance decaying to $\bar{p}\pi^+\pi^-$ or $p\pi^+\pi^-$ would be inconsistent with the conclusion that reaction (1) is dominated by nearly 100% $\bar{\Delta}^{--}\Delta^{++}$ production. However, in a recent study of the reaction $\bar{p}p(n)\to\bar{p}p\pi^+\pi^-(n)$ at 2.8 GeV/c by Bacon *et al.*,[4] effects were reported in the $\bar{p}\pi^+\pi^-$ and $p\pi^+\pi^-$ mass distributions. These effects were assigned masses of 1400±10 MeV and widths of 80±20 MeV. It was also reported that resonance production ($\bar{\Delta}^{--}\Delta^{++}$ plus some single-resonance production) accounts for only 72% of the events at 2.8 GeV/c. Since these findings are not in agreement with the 2.7- and 2.9-GeV/c results, an investigation was done[11] to determine whether the $\bar{p}\pi^+\pi^-$ and $p\pi^+\pi^-$ invariant-mass distributions at 2.7 and 2.9 GeV/c could be explained by the double-isobar OPE model. The conclusion was that the model does give an adequate representation of the data and that reaction (1) proceeds essentially 100% through the $\bar{\Delta}^{--}\Delta^{++}$ channel at both momenta. Ferbel *et al.*[6] found that a similar calculation gives an acceptable representation of the data for reaction (1) at 3.28 and 3.66 GeV/c. The calculations are given in Ref. 11 and are not repeated here. Since the 2.4-GeV/c data were not shown in Ref. 11, they are presented here (along with the 2.9-GeV/c data for completeness) in Fig. 8.

The data having both $\bar{p}\pi^-$ and $p\pi^+$ invariant masses in 1236±115 MeV and in the more restricted region 1236±50 MeV are shown in Figs. 8(b) and 8(d) at 2.4 and 2.9 GeV/c, respectively. The corresponding calculated distribution is shown normalized to the data in each case. The agreement is seen to be quite good at 2.9 GeV/c, and is also good at 2.7 GeV/c.[11] However, the model does not represent the data well at 2.4 GeV/c.

The $\bar{p}\pi^+\pi^-$ and $p\pi^+\pi^-$ mass distributions were also examined for events having *either* the $\bar{p}\pi^-$ or $p\pi^+$ mass outside the Δ region, and for events having *both* $\bar{p}\pi^-$ and $p\pi^+$ masses outside the Δ region. While the numbers of events meeting these requirements are limited, both of these restrictions yielded $\bar{p}\pi^+\pi^-$ and $p\pi^+\pi^-$ mass distributions at 2.4 GeV/c which lacked the apparent enhancement in the 1400–1520-MeV region. Apparently this effect is associated with the double-resonance production. Further, the prediction of phase space is peaked well above 1520 MeV, which argues against the effect being due to a large nonreasonant background.

V. CONCLUSIONS

The cross section for reaction (1) is 1.50±0.07 mb at 2.4 GeV/c and 2.57±0.10 mb at 2.9 GeV/c. The data are consistent with nearly 100% double-resonance production at 2.4, 2.7, and 2.9 GeV/c.

Reaction (1) is peripheral at both 2.4 and 2.9 GeV/c, the distribution of the c.m. scattering angle being peaked near $\cos\theta_p=1$; this peak becomes sharper with increasing beam momentum. Wolf[16] has shown that this effect is consistent with the double-isobar OPE model. In contrast, the decay angular distributions are not well predicted by the model.

The $\rho_{1,1}$ spin-density matrix element has a strong dependence on the square of the four-momentum transfer, falling at each momentum reported here from a value of about 0.5 at $\Delta^2=0$ to about 0.2 in the region $\Delta^2\sim0.6$ (GeV/c)^2, then rising again for larger Δ^2. A similar behavior is seen in the data at higher momenta, where it has been explained in terms of the OPE model with absorption.[20] No correlation in the $\bar{\Delta}^{--}$ and Δ^{++} production is indicated by the joint spin-density matrix elements reported here.

The double-isobar OPE model gives a good representation of the Δ^2 distribution, but a somewhat less satisfying prediction of the $\bar{p}\pi^-$ and $p\pi^+$ invariant-mass distributions. The predictions for both distributions are better at 2.9 GeV/c than at 2.4 GeV/c. The predictions of the $\bar{p}\pi^+\pi^-$ and $p\pi^+\pi^-$ invariant-mass distributions are acceptable at 2.9 GeV/c; but are not at all good at 2.4 GeV/c. It is clear that the form-factor OPE model, though accurate in some of its predictions, is not completely adequate for describing the data.[22]

ACKNOWLEDGMENTS

The authors express their gratitude to the staffs of the Alternating Gradient Synchrotron and the 31-in. bubble chamber at Brookhaven National Laboratory. The assistance of Dr. H. N. Brown of BNL with the operation of the beam he designed is most gratefully acknowledged. The work of the scanning, measuring, and programming staffs at the Ames Laboratory is also gratefully acknowledged. The assistance of Dr. T. L. Schalk on the data acquisition with the on-line measuring system is also appreciated. C. H. Hafen provided valuable help in checking the spin-density matrix element formulas.

[22] Including absorption in the OPE model calculations improves the agreement between the theoretical and experimental values of the spin-density matrix elements, but still does not perfectly reproduce the data (see CLK).